Simultaneous determination of built-in voltage and charge carrier mobility in organic diodes from light intensity dependent current–voltage characteristics

Fobao Huang[1]**, Yingquan Peng**[1,2]**, Kun Xu**[1]**, Wenli Lv**[2]**, Sunan Xu**[1,2]**,
Ying Wang**[3]**, Ying Tang**[2]**, Yi Wei**[2]**, Yuhuan Yang**[2] **and Guohan Liu**[1,4]

[1] Institute of Microelectronics, School of Physical Science and Technology, Lanzhou University,
Lanzhou 730000, People's Republic of China
[2] College of Optical and Electronic Technology, China Jiliang University, Hangzhou 310018,
People's Republic of China
[3] College of Information Engineering, China Jiliang University, Hangzhou 310018,
People's Republic of China
[4] Institute of Sensor Technology, Gansu Academy of Sciences, Lanzhou 730000,
People's Republic of China

E-mail: yqpeng@lzu.edu.cn (Y Peng) and gh.liu@gsas.ac.cn (G Liu)

CrossMark

Abstract

Built-in voltage (V_{bi}) and charge carrier mobility are essential parameters of organic diodes,
such as organic photodiodes, organic light-emitting diodes and organic solar cells. The
existing methods for charge carrier mobility measurement require either expensive equipment,
or stringent sample preparation. We demonstrate a method that simultaneously determines
the V_{bi} and charge carrier mobility in organic photodiodes and solar cells from incident light
intensity dependent current–voltage characteristics. The V_{bi} is determined from the saturation
open-circuit voltage, while the charge carrier mobility from the space-charge limited
photocurrent. The V_{bi} for organic diodes, 'ITO/copper phthalocyanine (CuPc)/2,9-dimethyl-
4,7-diphenyl-1,10-phenanthroline (BCP)/Al', 'ITO/ lead phthalocyanine (PbPc)/BCP/Al',
'ITO/CuPc/C_{60}/BCP/Al', and 'ITO/PbPc/C_{60}/BCP/Al', were measured to be 0.583 ± 0.019,
0.458 ± 0.002, 0.605 ± 0.009 and 0.538 ± 0.004 V, respectively; the hole mobility of
CuPc and PbPc thin films were measured to be $(1.383 \pm 0.367) \times 10^{-6}$ cm^2 V^{-1} s^{-1} and
$(3.675 \pm 0.887) \times 10^{-6}$ cm^2 V^{-1} s^{-1}, respectively. The measured values for V_{bi} and carrier
mobility coincide with related experimental results reported in other literature.

Keywords: built-in voltage, charge carrier mobility, organic diode

(Some figures may appear in colour only in the online journal)

1. Introduction

Most organic diodes exhibit non-zero built-in voltages, V_{bi}.
One reason for this is that optimal performance of organic
light-emitting diodes (OLEDs) generally requires that the
energy barrier for hole transport at the anode, and the energy
barrier for electron transport at the cathode be as low as pos-
sible, which leads to that different materials for electron and
hole contact are used for most optimized devices; the other
is that there exists vacuum level discontinuity [1] in many
metal/organic and organic/organic interfaces. Built-in voltage
is an important parameter for organic devices, especially for

organic diodes, since it influences the internal electric field profile in the devices, determines the onset voltage of OLEDs and also gives an upper limit for the open circuit voltage [2] and hence the efficiency of organic solar cells. In addition, V_{bi} can be used to determine the energy barrier at the two contacts via the relation $qV_{bi} = \phi_{ha} - \phi_{hc}$ [3, 4], where ϕ_{ha} and ϕ_{hc} are the hole-injection barriers at the two electrodes. Therefore the correct determination of the built-in voltage is essential to better understand the potential of a given material combination used as the active layer of organic devices. Conventionally, saturation photovoltage method [5–7], electro absorption [8, 9], steady-state current–voltage measurements [10] and Mott-Schottky method [11] are used for V_{bi} measurement, among which the saturation photovoltage method has the advantage of being simple and reliable.

Mobility is of great importance for organic semiconductor thin films. For mobility measurement, time of flight (TOF) [12], space-charge limited (SCL) current [13, 14], charge extraction by linearly increasing voltage (photo-CELIV) [15, 16] and impedance spectroscopy (IS) [17] are frequently used. Except SCL, the existing methods require either expensive equipment like pulsed laser, or sophisticate setup. Although simple, SCL method requires that the injection contact for the to be measured charge carrier must be Ohmic, which limit its use for measuring hole mobility with low lying HOMO levels, or electron mobility with high lying LUMO levels.

In this paper, with photosensitive organic molecules, copper phthalocyanine (CuPc) and lead phthalocyanine (PbPc) as example, we propose and demonstrate a simple and inexpensive method that simultaneously determines the built-in voltage and carrier mobility of organic diodes from light intensity dependent current–voltage (*IV*) characteristics. In this method, the V_{bi} is determined from the saturation open-circuit voltage, while the carrier mobility is extracted from the SCL photocurrent. Compared to the conventional methods, like TOF, photo-CELIV and IS for the measurement of carrier mobility, this method has the advantage of cheap and simple measurement setup. For example, in TOF method, charge carriers are generated via a short laser pulse (~ns), and the time needed for these charge carriers to drift to the opposite electrode is measured. In its measurement setup, expensive equipments like pulsed laser, high speed amplifier and large band-gap storage oscilloscope are included. While for the measurement setup of present method, only cheap apparatus like laser diode, light intensity meter, and conventional voltage and current source meters for characterization of current–voltage curves are needed.

2. Experimental

Organic semiconductor material CuPc was purchased from J&K Chemical Ltd, PbPc from Sigma-Aldrich Ltd, C_{60} from Luminescence Technology Co. Ltd, Taiwan, and 2,9-dimethyl-4,7-diphenyl-1,10-phenanthroline (BCP) from Jilin OLED Co. Ltd, respectively, and used as received. The configurations of organic diodes are presented in the insets of figures 1(a), 5(a) and 7. The organic diodes were fabricated according to the following procedures. A 30 Ω/square patterned indium-tin oxide

(ITO) coated glass was used as the substrate and the bottom electrode. The substrate was first ultrasonically cleaned by acetone, ethanol and de-ionized water, and dried by blowing high-pure N_2 and baked in an vacuum oven with temperature of 60 °C for 30 min and then UV ozone treated. Next, CuPc (or PbPc) was firstly deposited onto the ITO substrate and sequentially C_{60}, BCP was thermally evaporated onto the aforementioned substrate and the evaporation rate was kept at 1–2 nm min^{-1}, monitored by a quartz crystal oscillator. After that, an aluminium (Al) thin film was thermally deposited on the top of organic films as the top electrode via a shadow mask. During all the materials deposition, the chamber pressure was kept at the value of less than 1.5×10^{-3} Pa. In photosensitive characteristic measurements, a central wavelength of 655 nm red light laser with power of 50 mW and a homemade measurement system were used. The Al electrode and ITO electrode are connected with the negative electrode and the positive electrode, respectively. For the illumination, different optical powers were achieved by inserting neutral filters with various transmittances in the light path and the whole measurements were performed in a vacuum below 10 Pa. Active areas of the devices were defined by the overlapping region of the ITO anode and Al cathode which is 4 mm^2 and all devices were deposited in the same batch.

3. Results and discussion

3.1. Determining built-in voltage of organic diodes from saturation open-circuit voltage

As the built-in voltage of a photovoltaic device, V_{bi}, set the upper limit of its open-circuit voltage, therefore, V_{bi} can be determined by the saturation value of the open-circuit voltage. Figure 1(a) shows the *IV* characteristics of the diodes with the structure of 'ITO/CuPc/BCP/Al' (CuPc layer thickness 200 nm) in the dark and under laser illumination at 655 nm. The device is rectifying in the dark, but under illumination a substantial open-circuit voltage is observed, and current flow is enhanced in reverse bias (ITO was held negative). The open-circuit voltage of this device is plotted as a function of incident intensity in figure 2, where it can be seen that the open-circuit voltage rises steeply at low intensities and slowly at high intensities, and finally saturates at around 0.5 V. Figure 3 shows the histogram of measured values from several samples, from which the V_{bi} was determined to be 0.583 ± 0.019 V.

The low limit of V_{bi} can be estimated by adopting the metal-insulator-metal (MIM) model (no band bending, no interface dipole). In this model, the V_{bi} of single layer organic diodes can be estimated from the workfunction of anode (W_a), the workfunction of cathode (W_c), LUMO and HOMO levels of the organic molecules from equation (1) [18, 19]:

$$V_{bi} = \frac{1}{q}\left[\text{Min}(W_a, \text{HOMO}) - \text{Max}(W_c, \text{LUMO})\right], \quad (1)$$

here q is elementary charge. For organic devices based on donor (D)/acceptor (A) heterojunction, the above equation can be modified as [19]:
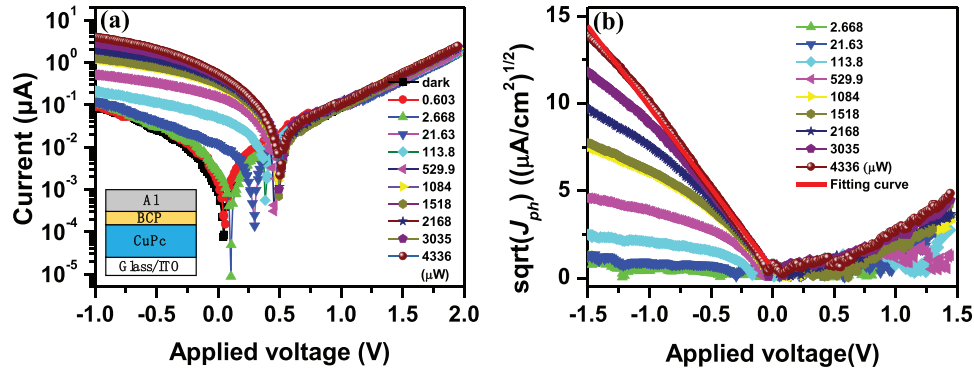
Figure 1. Characteristics of ITO/CuPc (200 nm)/BCP (15 nm)/Al diodes under 655 nm light illumination at different intensities: (a) *IV* curves; (b) $\sqrt{j_{ph}} \sim V$ curves.
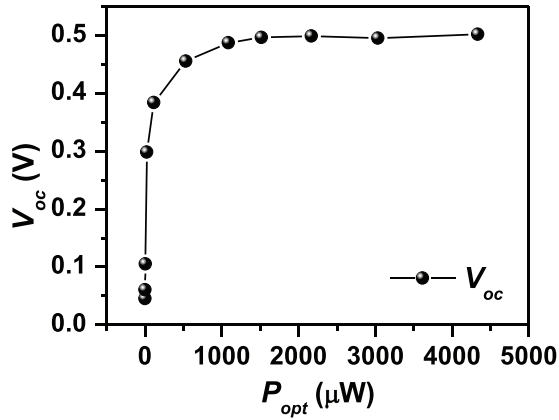

Figure 2. The open-circuit voltage, V_{oc}, of the device extracted from figure 1 as a function of the incident optical power.
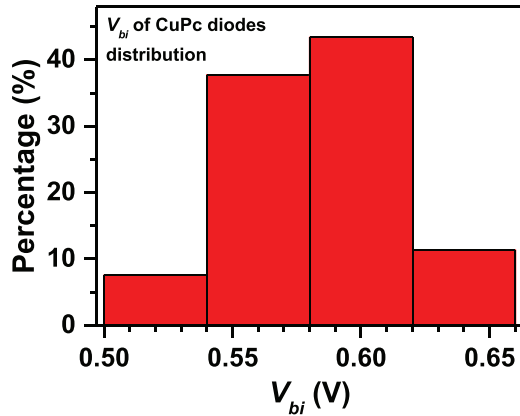

Figure 3. Histogram of measured built-in voltage of CuPc diodes with the structure of 'ITO/CuPc/BCP/Al'.

$$V_{bi} = \frac{1}{q} [\text{Min}(W_a, \text{HOMO}_D, \text{HOMO}_A) - \text{Max}(W_c, \text{LUMO}_D, \text{LUMO}_A)]. \qquad (2)$$

The electron transport across the BCP layer occurs mainly through gap states induced by the thermalization of the hot Al atoms during the deposition process, the high-density gap states were formed in BCP because of charge transfer between BCP molecules and Al atoms [20, 21]. This can also be found
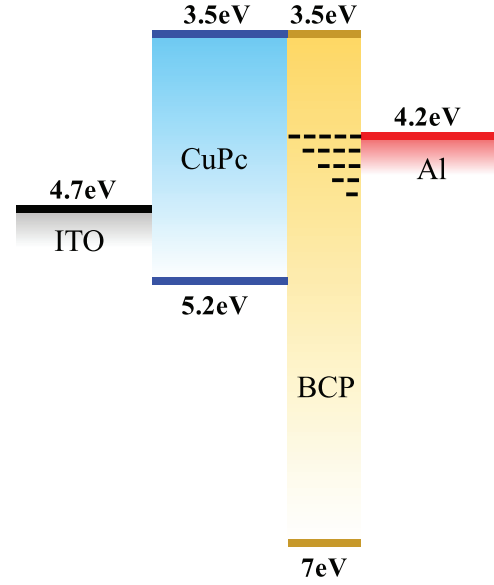

Figure 4. Schematic energy diagram of the diodes with the structure of ITO/CuPc/BCP/Al.

in recent studies about BCP/metal interface [22]. The work-function of BCP/Al bilayer cathode is considered to be 4.2 eV, same as Al [21]. Figure 4 shows the energy levels of the diodes based on the data from [23, 24]. Taken the workfunction of ITO be 4.7 eV [25], the V_{bi} in MIM model is calculated from equation (1) to be 0.5 V. The measured V_{bi} of 0.583 ± 0.019 V is comparable with this value. PbPc is a photosensitive molecule with optical absorption extending to near infrared, and is therefore important for photodiodes [26] and photosensitive organic field-effect transistors [27, 28], and solar cells [29]. Figure 5(a) shows the *IV* characteristics of organic diodes with the structure of 'ITO/PbPc(200 nm)/BCP(15 nm)/Al', the V_{bi} is determined to be 0.458 ± 0.002 V from the saturation photovoltage.

The energy level diagram for diode 'ITO/CuPc(50 nm)/C$_{60}$(50 nm) /BCP(15 nm)/Al' is shown in figure 6 [24], from which a reference value of V_{bi} was estimated from equation (2) of MIM model to be 0.2 eV. Figure 7 shows the *IV* characteristics of organic diodes with the structure of 'ITO/CuPc(50 nm)/C$_{60}$(50 nm) /BCP(15 nm)/Al' under different illumination intensities, the V_{bi} is determined to be 0.605 ± 0.009 V from

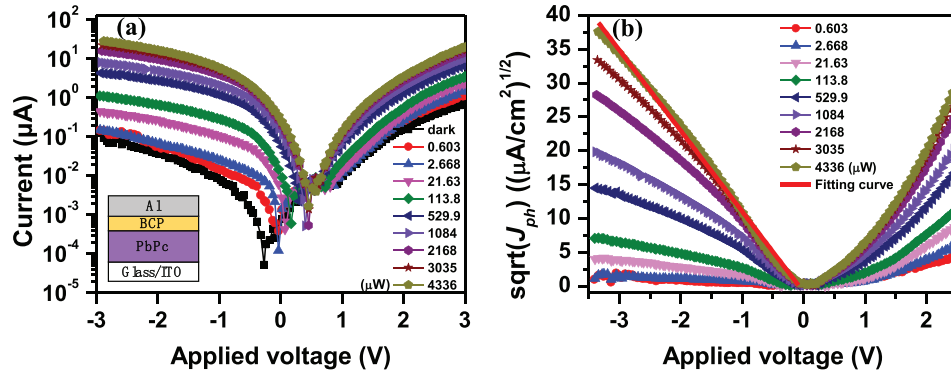J. Phys. D: Appl. Phys. **50** (2017) 205106

F Huang *et al*

Figure 5. Characteristics of ITO/PbPc (200 nm)/BCP (15 nm)/Al diodes under 655 nm light illumination at different intensities: (a) *IV* curves; (b) $\sqrt{j_{ph}} \sim V$ curves.
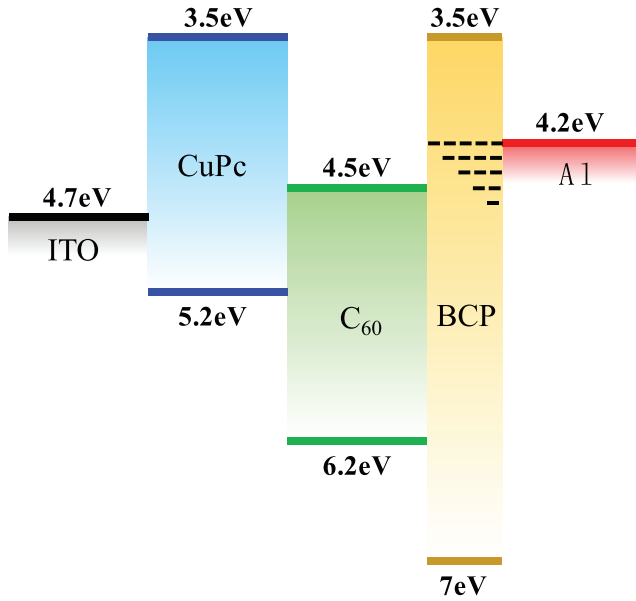

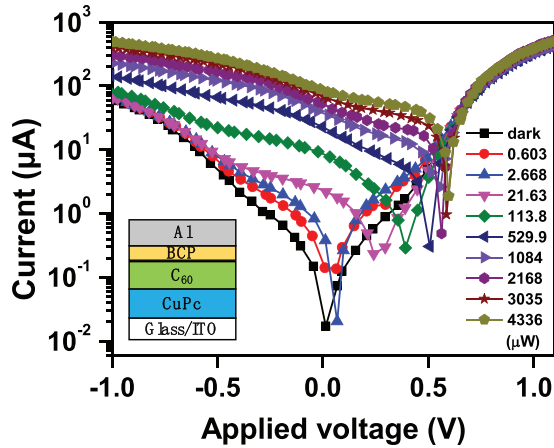**Figure 6.** Schematic energy diagram of the diodes with the structure of ITO/CuPc/C$_{60}$/BCP/Al.

Figure 7. *IV* curves for an ITO/CuPc (50 nm)/C$_{60}$ (50 nm)/BCP (15 nm)/Al device, illuminated by 655 nm light from a diode laser at different intensities.

the saturation photovoltage, which is reasonable well above not only the estimated minimal value of 0.2 eV, but also the open-circuit voltage of 0.46 V for CuPc/C$_{60}$ heterojunction based solar cells [30].

We also measured the V_{bi} of diodes with the structure of 'ITO/PbPc(50 nm)/C$_{60}$(50 nm)/BCP(15 nm)/Al'. The LUMO and HOMO of PbPc were reported to be 3.9 and 5.2 eV [29], respectively, substituting them into that of CuPc in the energy level diagram of figure 6, a value of 0.2 V was obtained for V_{bi} from equation (2) of the MIM model. Figure 7 shows the *IV* characteristics of the diodes under illumination of different intensities, the V_{bi} was determined to be 0.538 $\pm$ 0.004 V from the saturation photovoltage, which is reasonable well above estimated value from the MIM model, as well as the reported open-circuit voltage of 0.51 V [31] and 0.46 V [29] for PbPc/C$_{60}$ based solar cells.

3.2. Extracting charge carrier mobility from SCL photocurrent in Schottky contacted organic diodes

The dissociation probability of an exciton increases exponentially with the local electric field. At zero bias voltage, the built-in voltage drops mainly at the CuPc/Al interface, and the electric field there is therefore stronger than in the rest regions (figure 8(a)). Under light illumination, the photo generated excitons diffuse all around, and a part of them reach the high electric region near the Al electrode, and dissociate there to form photo holes and photo electrons. At the positive bias, the applied electric field is in opposite with the internal electric field near the Schottky contact (figure 8(b)), and the field there is thus weakened, which results in low dissociation probability, this is the reason why the photocurrent density is much smaller than the case of inverse bias, as shown in figure 1. At the reverse bias, the applied electric field is parallel with the internal electric field near the Schottky contact, and the electric field there is thus strengthened (figure 8(c)), resulting in enhancement in exciton dissociation probability. The photo holes generated near the BCP/Al cathode drift towards the ITO electrode, while the photo electrons are collected by the BCP/Al electrode. For moderate reverse biases, the contribution to the current flow in the device is dominantly from the drift of photo holes across the CuPc layer towards the ITO electrode, characterized by the space charge limited current conduction, described as follows:

$$j_{ph} = \frac{9}{8}\varepsilon_0\varepsilon_r\mu\frac{(V - V_{bi})^2}{d^3}, \qquad (3)$$

J. Phys. D: Appl. Phys. **50** (2017) 205106
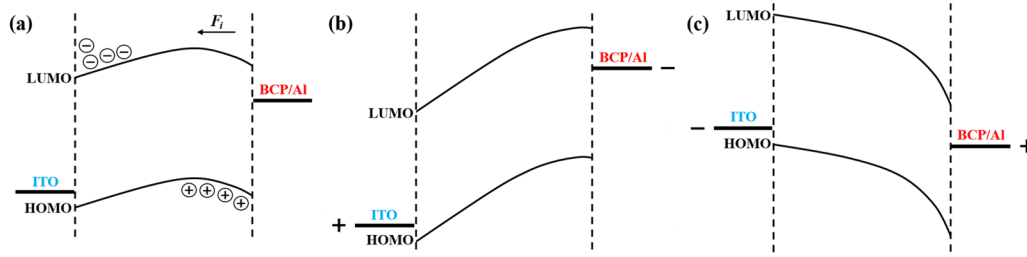
F Huang *et al*

Figure 8. Energy level diagram of organic diodes under different voltage biases conditions. (a) At zero bias, there is a built-in electric field; (b) at positive biases, the applied electric field is opposite in direction with the built-in electric field, which weakened the electric field near the cathode; (c) at negative biases, the applied electric field has the same direction with the built-in electric field, which strengthens the electric field near the cathode.
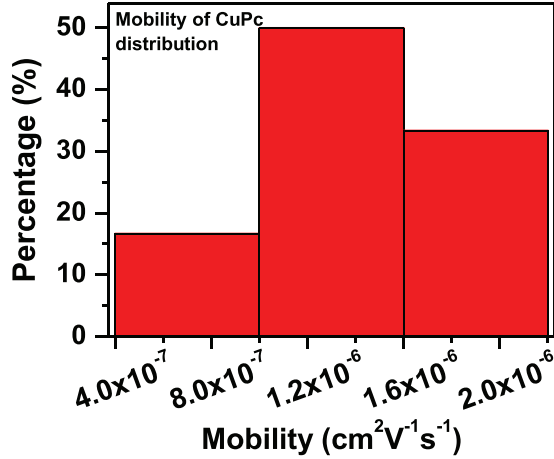

Figure 9. Histogram of measured hole mobility of CuPc thin film.

$$\sqrt{j_{ph}} = \sqrt{\frac{9\varepsilon_0\varepsilon_r\mu}{8d^3}} (V - V_{bi}). \tag{4}$$

Taken the dielectric constant of CuPc film be $\varepsilon_r = 4.69$ [32], $d = 200$ nm, the mobility μ of CuPc film can be extracted from the slop of equation (4) by fitting measured $\sqrt{j_{ph}} \sim V$ values with equation (4), as shown in figure 1(b). Figure 9 shows the histogram of measured hole mobility for several device samples, from which a value of $(1.383 \pm 0.367) \times 10^{-6}$ cm^2 V^{-1} s^{-1} was obtained, which is within the range of reported values from 1.03×10^{-7} cm^2 V^{-1} s^{-1} [33] to 7.87×10^{-5} cm^2 V^{-1} s^{-1} [34] in other literature.

Figure 5(b) shows the $\sqrt{j_{ph}} \sim V$ curves of the diode 'ITO/PbPc/BCP/Al' from figure 5(a). For high illumination intensities, the curves in the range of -0.5 to -1.5 V are nearly straight lines and the slop saturates with the light intensity increasing. Taken the dielectric constant of PbPc be 3.39 [35], a hole mobility of $\mu = (3.675 \pm 0.887) \times 10^{-6}$ cm^2 V^{-1} s^{-1} was calculated by equation (4) from the curve under 4336 μW illumination. This value is in good agreement with that reported in [36] $(1.01 \times 10^{-6}$ cm^2 V^{-1} s$^{-1})$ and [37] $(6.05 \times 10^{-6}$ cm^2 V^{-1} s$^{-1})$.

4. Conclusions

A method that simultaneously determines the V_{bi} and charge carrier mobility in organic photodiodes and solar cells from incident light intensity dependent *IV* characteristics is demonstrated. The V_{bi} is determined from the saturation photovoltage, while the charge carrier mobility from the SCL photocurrent. The V_{bi} for organic diodes, 'ITO/CuPc/BCP/Al', 'ITO/PbPc/BCP/Al', 'ITO/CuPc/C$_{60}$/BCP/Al', and 'ITO/PbPc/C$_{60}$/BCP/Al', were measured to be 0.583 ± 0.019 V, 0.458 ± 0.002 V, 0.605 ± 0.009 V and 0.538 ± 0.004 V, respectively; the hole mobility of CuPc and PbPc thin films were measured to be $(1.383 \pm 0.367) \times 10^{-6}$ cm^2 V^{-1} s^{-1} and $(3.675 \pm 0.887) \times 10^{-6}$ cm^2 V^{-1} s^{-1}, respectively. These measured values for V_{bi} and carrier mobility are in good agreement with that reported in other literature.

References

[1] Ishii H and Seki K 1997 *IEEE Trans. Electron Devices* **44** 1295–301
[2] Rauh D, Wagenpfahl A, Deibel C and Dyakonov V 2011 *Appl. Phys. Lett.* **98** 133301–3
[3] Parish C M and Russell P E 2006 *Appl. Phys. Lett.* **89** 192103–8
[4] Campbell I H, Hagler T W, Smith D L and Ferraris J P 1996 *Phys. Rev. Lett.* **76** 1900–3
[5] Ikram I M, Rabinal M K and Mulimani B G 2009 *Eur. J. Phys.* **30** 127–34
[6] Malliaras G G, Salem J R, Brock P J and Scott J C 1998 *J. Appl. Phys.* **84** 1583–7
[7] Marks R N, Halls J J M, Bradley D D C, Friend R H and Holmes A B 1994 *J. Phys.: Condens. Matter* **6** 1379
[8] Bodrozic V, Roberts M, Phillips N and Burroughes J H 2007 *J. Appl. Phys.* **101** 084507–9
[9] Hoven C V, Peet J, Mikhailovsky A and Nguyen T Q 2009 *Appl. Phys. Lett.* **94** 033301–3
[10] Van Mensfoort S L M, Vulto S I E, Janssen R A J and Coehoorn R 2008 *Phys. Rev.* B **78** 085208
[11] Nolasco J C, Sánchezdíaz A, Cabré R, Ferréborrull J, Marsal L F, Palomares E and Pallarès J 2010 *Appl. Phys. Lett.* **97** 2818–23
[12] Mazur L, Castiglione A, Ocytko K, Kameche F, Macabies R, Ainsebaa A, Kreher D, Heinrich B, Donnio B and Sanaur S 2014 *Org. Electron.* **15** 943–53
[13] Blom P W M, de Jong M J M and Vleggaar J J M 1996 *Appl. Phys. Lett.* **68** 3308–10
[14] Bozano L, Carter S A, Scott J C, Malliaras G G and Brock P J 1999 *Appl. Phys. Lett.* **74** 1132–4

J. Phys. D: Appl. Phys. **50** (2017) 205106

F Huang *et al*

[15] Juska G, Arlauskas K, Viliunas M and Kocka J 2000 *Phys. Rev. Lett.* **84** 4946–9

[16] Mozer A J, Sariciftci N S, Lutsen L, Vanderzande D and Westerling M 2005 *Appl. Phys. Lett.* **86** 112103–4

[17] Tang Y, Peng Y, Sun L, Wei Y and Xu S 2015 *Europhys. Lett.* **112** 17007

[18] Peng Y Q, Meng W M, Wang R S, Ma C Z, Li X S, Xie H W, Li R H, Zhao M, Yuan J T and Wang Y 2009 *Appl. Surf. Sci.* **255** 8010–3

[19] Wang Y, Ma C, Wang R, Li R and Peng Y 2011 *J. Optoelectron. Adv. Mater.* **13** 165

[20] Sun X, Di C and Liu Y 2010 *J. Mater. Chem.* **20** 2599–611

[21] Zhuang T, Su Z, Liu Y, Chu B, Li W, Wang J, Jin F, Yan X, Zhao B and Zhang F 2012 *Appl. Phys. Lett.* **100** 243902–4

[22] Luo X, Li Y, Lv W, Zhao F, Sun L, Peng Y, Wen Z, Zhong J and Zhang J 2015 *Nanotechnology* **26** 035201

[23] Matsuo Y, Son D, Shimoi Y and Marumoto K 2014 *Chem. Phys. Lett.* **607** 29–33

[24] Zhang G, Li W, Chu B, Chen L, Yan F, Zhu J, Chen Y and Lee C S 2009 *Appl. Phys. Lett.* **94** 143302–3

[25] Noh S, Kim S, Yang J, Lee C and Kim J Y 2008 *J. Korean Phys. Soc.* **5380** 1551–5

[26] Zhao F, Luo X, Liu J, Du L, Lv W, Sun L, Li Y, Wang Y and Peng Y 2016 *J. Mater. Chem.* C **4** 815–22

[27] Li Y, Zhang J, Lv W, Luo X, Sun L, Zhong J, Zhao F, Huang F and Peng Y 2015 *Synth. Met.* **205** 190–4

[28] Li Y, Lv W, Luo X, Sun L, Zhao F, Zhang J, Zhong J, Huang F and Peng Y 2015 *Org. Electron.* **26** 186–90

[29] Dai J, Jiang X, Wang H and Yan D 2007 *Appl. Phys. Lett.* **91** 253503

[30] Lo M F, Ng T W, Lai S L, Fung M K, Lee S T and Lee C S 2011 *Appl. Phys. Lett.* **99** 033302–3

[31] Shim H S, Kim H J, Ji W K, Kim S Y, Jeong W I, Kim T M and Kim J J 2012 *Proc. SPIE* **8477** 472–6

[32] Gordan O D, Friedrich M and Zahn D R T 2004 *Org. Electron.* **5** 291–7

[33] Mahapatro A K and Ghosh S 2007 *J. Appl. Phys.* **101** 034318

[34] Hung L S and Mason M G 2001 *Appl. Phys. Lett.* **78** 3732–4

[35] Sharma G D, Choudhary V S and Roy M S 2007 *Sol. Energy Mater. Sol. Cells* **91** 1087–96

[36] Sharma G D, Choudhary V S, Janu Y and Roy M S 2007 *Mater. Sci.* **25** 1173–91

[37] Ahmad A and Collins R A 1991 *Phys. Status Solidi* **123** 201–11